 MCB, vol.7, no.1, pp.1-11, 2010

A Computational Model for Cortical Endosteal Surface Remodeling Induced by Mechanical Disuse

He Gong[*,†] **and Ming Zhang**[‡]

Abstract: In mechanical disuse conditions associated with immobilization and microgravity in spaceflight, cortical endosteal surface moved outward with periosteal surface moving slightly or unchanged, resulting in reduction of cortical thickness. Reduced thickness of the shaft cortex of long bone can be considered as an independent predictor of fractures. Accordingly, it is important to study the remodeling process at cortical endosteal surface. This paper presents a computer simulation of cortical endosteal remodeling induced by mechanical disuse at the Basic Multicellular Units level with cortical thickness as controlling variables. The remodeling analysis was performed on a representative rectangular slice of the cross section of cortical bone volume. The pQCT data showing the relationship between the duration of paralysis and bone structure of spinal cord injured patients by Eser et al. (2004) were used as an example of mechanical disuse to validate the model. Cortical thickness, BMU activation frequency, mechanical load and principal compressive strain for tibia and femur cortical models were simulated. The effects of varying the mechanical load and maximum BMU activation frequency were also investigated. The cortical thicknesses of femur and tibia models were both consistent with the clinical data. Varying the decreasing coefficient in mechanical load equation had little effect on the steady state values of cortical thickness and BMU activation frequency. However, it had much effect on the time to reach steady state. The maximum BMU activation frequency had effects on both the steady state value and the time to reach steady state for cortical thickness and BMU activation frequency. The computational model for cortical endosteal surface remodeling developed in this paper can be further used to quantify and predict the effects of mechanical factors and biological factors on cortical thickness and help us to better understand the relationship between bone morphology and mechanical as well as biological environment.

Keyword: Remodeling; Cortical bone; Endosteal surface; Mechanical load; Basic Multicellular Unit

1 Introduction

The skeleton is made up of cortical bone and trabecular bone. Cortical bone, also known as compact or lamellar bone, forms the thin outer shell in the long bones and the major portion of the cortex of other bones. Trabecular bone is also known as spongy or cancellous bone. It is made of a network of intersecting plates and rods (trabeculae) within the cortex, and serves as the supportive infrastructure of the bone.

Throughout life, bone is constantly resorbed and new bone is formed by a process called bone remodeling, which is performed by groups of osteoblasts and osteoclasts organizing into Basic Multicellular Units (BMUs). About 5% of the bone mass is remodeled by about 2 million BMUs in the human skeleton at any time. The renewal rate for bone is about 4% per year for cortical bone and 20% per year for trabecular bone (Ganong 2005).

Osteoporosis is a systematic skeletal disease characterized by low bone mass and micro-

[*] Department of Health Technology and Informatics, The Hong Kong Polytechnic University, Hung Hom, Kowloon, China.

[†] Department of Mechanics, Jilin University, Changchun, China

[‡] Corresponding author. Tel: (852)2766 4939; Fax (852) 2362 4365; Email: htmzhang@polyu.edu.hk

architectural deterioration, with a consequent increase in bone fragility and susceptible to fracture. Structural integrity of trabecular bone is impaired and cortical bone becomes more porous and the cortex becomes thinner (Slade et al., 2005; Ritzel et al., 1997). Skeletal disuse, whether due to microgravity caused by spaceflight, prolonged bed rest, paralysis, localized stress shielding following arthroplasty, or cast immobilization may lead to bone loss in humans, as well as laboratory animals (LeBlanc et al. 1998; Prince et al., 1988; Paga et al., 1991). Aging, estrogen deficiency, and drug treatments are known as biological factors.

Some researchers built computational model for trabecular bone at BMUs level to theoretically analyze of the contributions of mechanical factors as well as biological factors on trabecular bone remodeling (Hernandez et al., 2001, 2003; Gong et al., 2006). These studies have led us to a better understanding of the trabecular bone-remodeling behavior and its importance for the biomechanical stability of the bone. However, the studies on the computational model for cortical bone remodeling are remarkable limited. Hazelwood et al. (2001) developed a mechanistic model for internal bone remodeling, which may be useful when examining the importance of transient responses for bone in disuse, and for investigating the role that fatigue damage removal plays in preventing or causing stress fractures. It has been shown that reduced thickness of the femoral shaft cortex is an independent predictor of hip fracture (Gluer et al., 1994). In mechanical disuse conditions associated with paralysis and microgravity caused by spaceflight it was found that cortical-endosteal surface moved outward at a significantly greater rate with periosteal surface moving slightly or unchanged, resulting in cortical thinning (Lang et al., 2004; Eser et al., 2004). Hence it is important to do computational simulation of cortical endosteal remodeling, which can be used to quantify and predict the effects of mechanical factors and biological factors on cortical thickness, and can help us to better understand the relationship between bone morphology and mechanical, as well as biological environment.

In this study, we develop a computational model at the BMU level for cortical endosteal remodeling. The pQCT data showing the relationship between the duration of paralysis and bone structure of spinal cord injured patients by Eser et al. (2004) were used as an example of mechanical disuse to validate the model.

2 Methods

A computer simulation of cortical endosteal surface remodeling was developed at the BMU level in this study. Six state variables and 9 constants included in the model were listed in Table 1 and Table 2. The remodeling analysis was performed on a representative rectangular slice of the cross-section of the cortical bone volume as shown schematically in Fig. 1.

2.1 Cortical thickness changes

An imbalance between bone resorption and refilling leads to changes in cortical thickness. The rate of change in cortical volume was assumed to be a function of the bone resorption rate ($Qr(x,t)$) and bone refilling rate ($Qf(x,t)$) for each BMU, and the density of resorbing and refilling BMUs/area ($N_R(x,t)$ and $N_F(x,t)$, respectively)

$$\frac{d\frac{h(t)\cdot l}{h_0\cdot l}}{dt} = Q_r(t)N_R(t) - Q_f(t)N_F(t) \tag{1}$$

where the resorption rate $Q_r(t)$ and the refilling rate $Q_f(t)$ were assumed to be linear in time: $Q_r(t) = \frac{A}{T_r}$ and $Q_f(t) = \frac{A}{T_f}$ with A representing the area of bone resorbed by each BMU. $h(t)$ was the cortical thickness at time t, l was the length of the representative rectangular slice and h_0 was the initial cortical thickness as shown in Fig. 1.

Hence

$$\frac{dh(t)}{dt} = h_0(Q_r(t)N_R(t) - Q_f(t)N_F(t)) \tag{2}$$

$N_R(t)$ and $N_F(t)$ were calculated as:

$$N_R(t) = \int_{t-T_r}^{t} f_a(t')dt' \tag{3}$$

$$N_F(t) = \int_{t-(T_r+T_i+T_f)}^{t-(T_r+T_i)} f_a(t')dt' \tag{4}$$

$f_a(t)$ was the BMU activation frequency.

Table 1: State variables in the model

	State variable
h	Cortical thickness (mm)
N_R	Number of resorbing BMUs (BMUs/mm^2)
N_F	Number of refilling BMUs (BMUs/mm^2)
fa	BMU activation frequency (BMUs/mm^2/day)
ε	Strain (μ, ε)
Φ	Mechanical stimulus (MPa)

BMU: Basic Multicellular Unit

Table 2: Constants in the model

	Constant	Norminal values in the example
A	Cross-sectional area of each BMU (mm^2)	2.84×10^{-2}[a]
T_r	Resorption period (days)	24[b]
T_i	Reversal period (days)	8[b]
T_f	Refilling period (days)	64[b]
$f_{a(\max)}$	Maximum BMU activation frequency (BMUs/mm^2/day)	0.299[c]
kb	Dose-response coefficient (Pa)	0.005759[c]
kc	Dose-response coefficient (Pa^{-1})	1129.493[c]
f_{a0}	Maximum BMU activation frequency (BMUs/mm^2/day)	4.8768×10^{-4}[d]
Φ_0	Initial Mechanical stimulus (Pa)	2258.986

[a:] based on Parfitt (1983)
[b:] from Hazelwood et al. (2001) based on several histomorphometric studies
[c:] parametrical sensitivity analyses were done for the coefficients to fit the curves within known experimental data ranges (Eser et al., 2004)
[d:] based on equation (5)

Table 3: The geometrical and mechanical conditions of the representative rectangular slices for femur and tibia cortical models

	Tibia	Femur	Remarks
Initial cortical thickness h_0 (mm)	5.84	3.33	From Eser et al. (2004).
Length l (mm)	1	1.64	The length of tibia model was chosen to guarantee a small slice and that of femur model was chosen such that both models occupied the same percentage of total cortical area, i.e. approximately 1.69%.
Initial area A_0 of the model (mm^2)	5.84	5.46	From equation $A_0 = h_0 \cdot l$.
Equilibrium strain ε_0 (μ ε)	500	500	From Beaupré et al. (1990) and Turner et al. (1997).
Porosity p_0 (%)	4.43	4.43	From Hazelwood et al. (2001). And from Eser et al. (2004), it was shown that no decrease in cortical BMD of the diaphyses with time after injury was found. Hence the cortical porosity in this analysis was held constant.
Elastic modulus E (MPa)	18000	18000	From the relationship between elastic modulus and porosity of cortical bone proposed by Currey (1988): $E = (23440 \times (1-p_0)^{5.74})MPa$.
Equilibrium load F_0 (N)	52.770	49.336	From equation $F_0 = \varepsilon_0 \cdot A_0 \cdot E$.

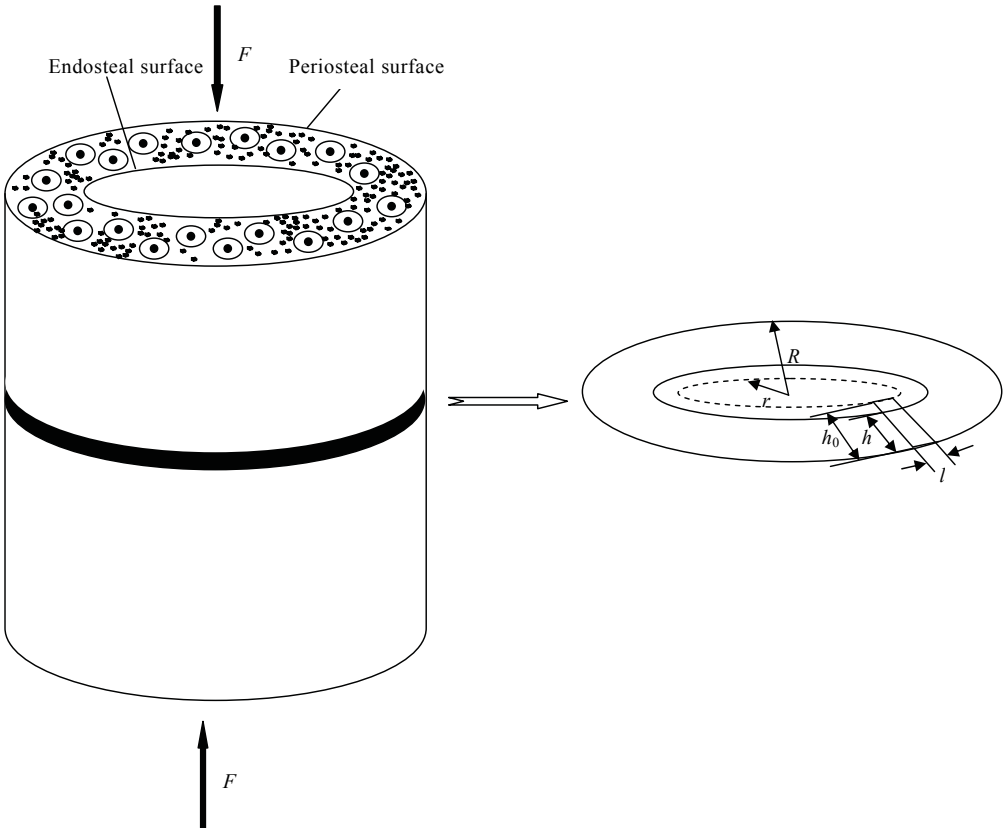

Figure 1: Schematic example of BMUs in a representative bone volume of cortical bone. The remodeling analysis was performed on a representative rectangular slice of the cross section of the cortical bone volume as shown schematically here. Bone volumes were assigned linearly elastic and isotropic material properties. Axial compressive loads are placed on the cortical bone volume. For simplification, the cortical bone volume was assumed to be cylindrical. r– Initial endosteal radius; R– Periosteal radius; l – Length of the representative rectangular slice; h – cortical thickness; h_0 – initial cortical thickness with $h_0 = R - r$.

2.2 BMU activation frequency

The relationship between BMU activation frequency and mechanical load was assumed to be sigmoidal, similar to the response found in pharmacological application (Hazelwood et al., 2001).

$$fa(t) = \frac{fa(\max)}{1 + e^{kb(\phi(t) - kc)}} \tag{5}$$

where $fa(\max) = 0.299\, BMUs/mm^2/day$, kb and kc were coefficients defining the slope and inflection point of the curve, respectively. Sensitivity analyses were done first for the coefficients in these functions to fit the curves within known experimental data ranges (Eser et al., 2004). $\phi(t)$ was mechanical stimulus, which was described by strain energy density (Mullender and Huiskes, 1995)

$$\phi(t) = \frac{1}{2} E(t) \cdot \varepsilon^2(t) \tag{6}$$

where $E(t)$ was the elastic modulus and $\varepsilon(t)$ was the mechanical strain.

2.3 Examples

The pQCT data showing the relationship between the duration of paralysis and bone structure of spinal cord injured patients by Eser et al. (2004) was used as an example of mechanical disuse. Eighty-nine motor complete spinal cord injured men (24 tetraplegics and 65 paraplegics) with a duration of paralysis of between 2 months and 50 years were included. The age range was 41.5±14.2 for all subjects. The reference group

comprised 21 healthy able-bodied men of the same age range.

The remodeling behaviors of cortical bone in the femur, as well as in the tibia were both simulated in this paper. The representative cross section of the femur cortical bone was located at 25% of total bone length from the distal end for the femur, and at 38% for the tibia as the locations of diaphyseal scans in Eser et al. (2004). For simplification, the cortical bone volume was assumed to be cylindrical and the endosteal surface and periosteal surface were assumed to be concentric circle (Fig. 1). The geometrical and mechanical conditions for the two cortical examples were shown in Table 3.

2.4 Loading conditions

The mechanical load in the disuse pattern of paralysis was assumed to decrease exponentially with the duration:

$$F(t) = F_0 \cdot e^{-t \cdot a} \tag{7}$$

with t = time (year), a was a decreasing coefficient, which was chosen such that the simulation results could be in accordance with experimental data ranges (Eser et al., 2004). F_0 was the equilibrium load.

Using a time-dependent approach (equations (1)–(7)), computer simulations of cortical endosteal remodeling processes in the femur, as well as in the tibia were performed from t = 0 day to t = 50 years to cover the course of the clinical investigation. The cortical thickness, BMU activation frequency, mechanical load and principal compressive strain were simulated. Effects of varying the mechanical load and maximum BMU activation frequency were also investigated.

3 Results

3.1 Simulation results of tibia and femur cortical models

Figure 2 shows the numerical outcomes of cortical thickness of the femur and tibia models. The simulated cortical bone thicknesses for both models were both consistent with the clinical data

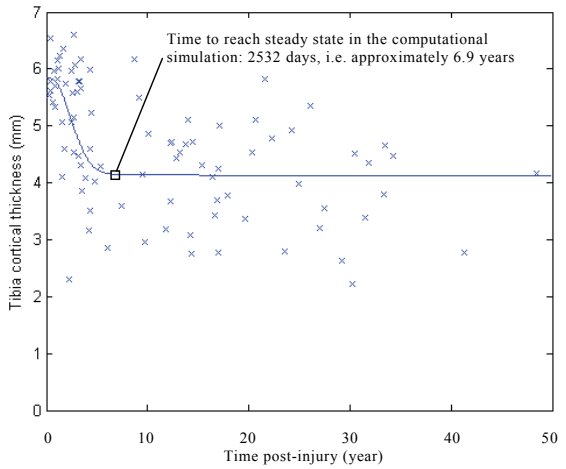

(a)

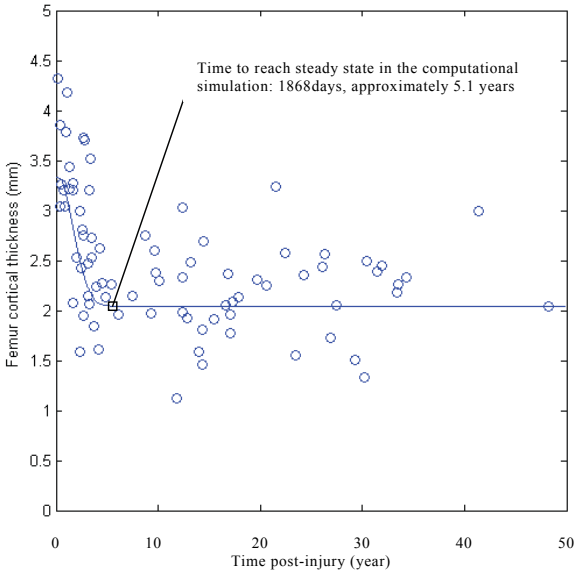

(b)

Figure 2: Simulation results of cortical thickness of tibia and femur models. The curves representing cortical thickness are the simulation outcomes. The data points show the clinical data measured by Eser et al. (2004). (a) Tibia model; (b) Femur model.

measured by Eser et al. (2004), which can be seen from the following aspects:

(1) The similarity of our numerical outcomes with clinical data can be seen directly from

fig. 2.

(2) The correlation coefficients between the clinical data points and the simulated values at the same time points were R^2=0.43 (p <0.001) for the femur model, and R^2=0.33 (p <0.001) for the tibia model.

(3) The times to reach steady state in the simulation were in agreement with the clinical investigation, i.e. approximately 5.1 years for femur cortical bone and 6.9 years for tibia cortical bone.

(4) The simulated steady state values of cortical thickness in both models were close to the clinical data. For the femur model, the simulated steady state value of cortical thickness was 2.038mm and the clinical data was 2.17mm with relative difference of 6.08%. For the tibia model, the simulated steady state value was 4.134mm and the clinical data was 3.94mm with relative difference of 4.92%.

Figure 3 shows the changes of mechanical load for both models. The mechanical load in the tibia model followed the equation $F(t) = F_{0\,tibia} \cdot e^{-0.2t}$ with t = time (year) and that in the femur model followed the equation $F(t) = F_{0\,femur} \cdot e^{-0.3t}$ with t = time (year). The values of $F_{0\,tibia}$ and $F_{0\,femur}$ are listed in Table 3, respectively. The effect of decreasing coefficient a in equation (7) on the simulation results will be shown later.

The changing patterns of BMU activation frequency and principal compressive strain on both models are shown in figure 4 and figure 5, respectively.

From fig. 3 mechanical load in the femur cortical bone decreased faster than that in the tibia cortical bone, hence the decrease of strain and mechanical stimulus was also faster (figure 5), and the BMU activation frequency in the femur cortical bone increased faster and reached a higher level in response to the faster mechanical disuse situation (figure 4). As a result, the femur cortical thickness decreased more and was faster to reach steady state value than the tibia model, which was in accordance with clinical observation.

Taking femur model as an example, effects of varying the mechanical load and the maximum BMU activation frequency were obtained as follows:

3.2 Effects of the decreasing coefficient in mechanical load equation

The effects of varying the decreasing coefficient a of mechanical load [equation (7)] on cortical thickness and BMU activation frequency were shown in figure 6. From the nature of exponential function of equation (7), a determines the decreasing speed and F_0 determines the initial and maximum value of the mechanical load, and the mechanical load is close to zero after a relative long period of time. Varying the decreasing coefficient had little effect on the steady state values of cortical thickness and BMU activation frequency. However, it had much effect on the time to reach steady state. With a increasing from 0.15 to 0.5, the time to reach steady state was significantly reduced.

3.3 Effects of the maximum BMU activation frequency

The effects of varying the maximum BMU activation frequency on cortical thickness and BMU activation frequency were shown in figure 7. The maximum BMU activation frequency had effects on both the steady state value and the time to reach steady state for cortical thickness, as well as BMU activation frequency. Decreases of the steady state cortical thickness and increases of BMU activation frequency were observed as the maximum BMU activation frequency increased. And the time to reach steady state also increased as the maximum BMU activation frequency increased.

4 Discussion

The observed adaptation of bone mass and architecture to the typical mechanical usage indicated that some mechanism existed for monitoring the mechanical usage and controlling bone modeling and remodeling activities (Forwood and Turner, 1995; Turner et al., 1994). Loads on

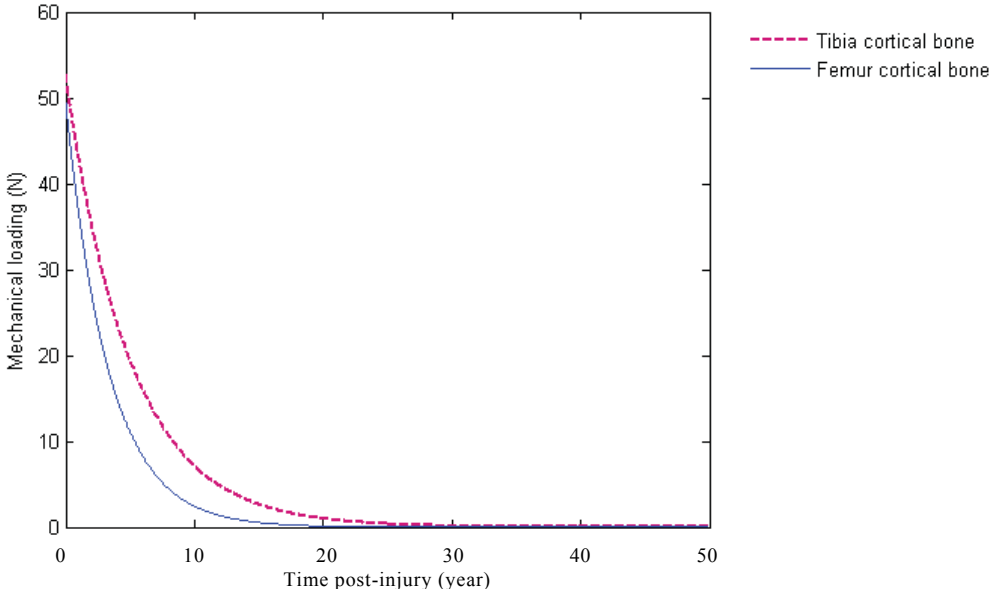

Figure 3: Changes of mechanical load for both models.

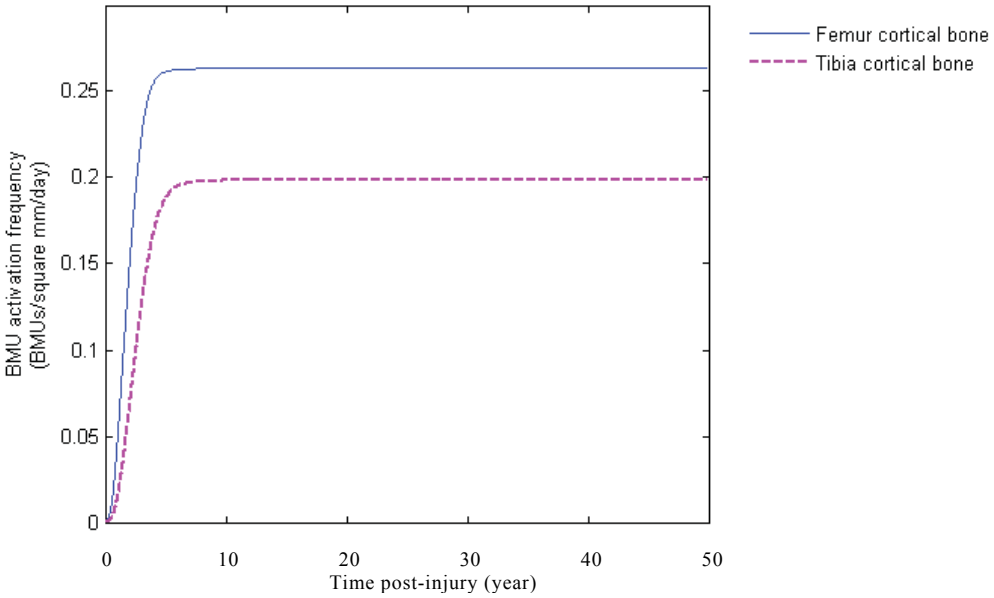

Figure 4: Changing patterns of BMU activation frequency in both models.

bones generated strain-dependent signals (Martin 2000; Jones et al., 1991). Frost (1983) used the minimum effective strain (MES) as threshold or mechanical set point to describe bone's adaptation to its mechanical environment. When dynamic strains stay below a lower remodeling threshold range (MESr), 'disuse-mode' remodeling removes bone next to marrow. That removal causes a 'disuse-pattern' osteopenia characterized by widened marrow cavities, cortical thinning, and normal or even slightly increased outside bone diameters (Frost 2000). This is the physiological basis for our computational simulation for cortical endosteal surface remodeling induced by mechanical disuse.

Eser et al. (2004) did not find decrease in cortical BMD of the diaphyses with time after injury. Besides, Feik et al. (1997) investigated the complete cross-sections from the femoral midshaft of 180 individuals aged 21-97 years and found that

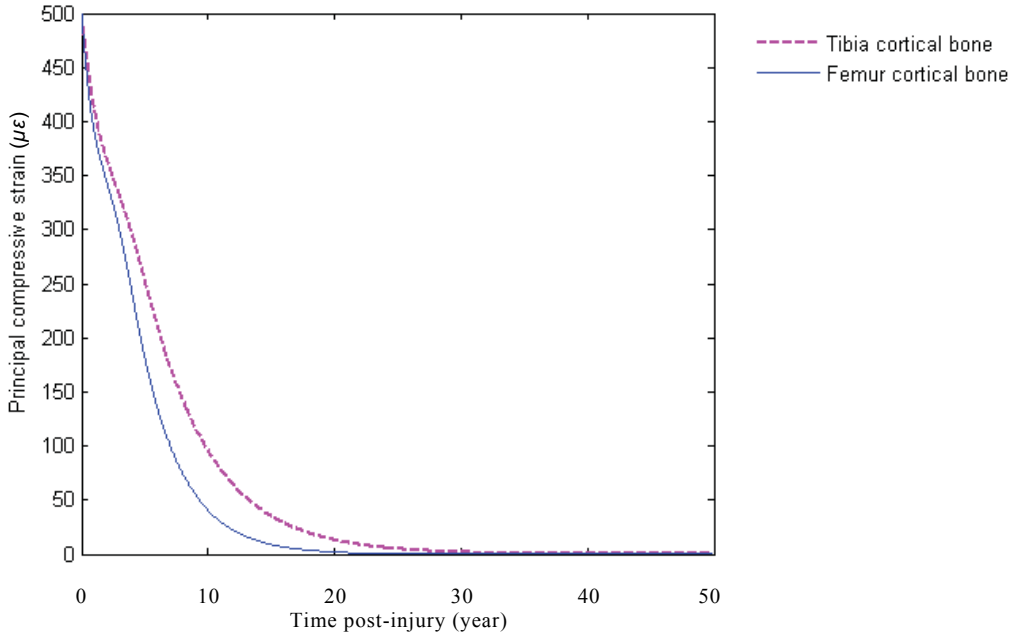

Figure 5: Changing patterns of principal compressive strain in both models.

male intracortical porosity changed little with aging from twenties to eighties. Hence it was reasonable to set the cortical thickness as state variable to control the remodeling process, while the cortical porosity was held constant in this analysis. An in vivo animal model of disuse osteopenia set up by Gross and Rubin (1995) suggested that disuse induced a uniform expansion of the endosteal envelop of the radius. Hence by conducting bone remodeling analysis on a representative rectangular slice of the cross section of the cortical bone volume, and setting the cortical thickness as control variable, the cortical endosteal surface remodeling can be simulated.

As femur and tibia are weight-bearing bones, whose main function is to withstand loads placed on them. Bone quality and quantity are closely related to the mechanical load conditions. For the paralyzed patients the loads on femur and tibia were significantly reduced, which resulted in significant reduction in cortical thickness of femur, as well as tibia. However, the speed and amount of cortical thickness reduction were not the same for both locations as indicted in the clinical investigation by Eser et al. (2004). By assuming a proper form of mechanical load and investigating the effects of varying the mechanical load and maximum BMU activation frequency, the simulated cortical thickness for the femur and tibia models can be both consistent with the clinical data. It is difficult to measure the mechanical loads placed on femur and tibia in vivo. Although we can not say for sure that the mechanical loads decrease exactly according to the equations we assumed in the process of paralysis, it can at least shed some light on the decreasing characteristics of mechanical load.

There was much difference in the remodeling behaviors between males and females. Feik et al. (1997) found that the introcortical porosity of females with the age of 60 years above was significantly greater than that of females in their twenties. The bone remodeling behaviors of females was influenced not only by mechanical load, but also biological factors such as aging and estrogen deficiency (Gong et al., 2006). In this case, for the quantification of cortical endosteal surface remodeling of females, a new remodeling scheme including both the cortical thickness and porosity as controlling variables, and their coupling factors needs to be further investigated.

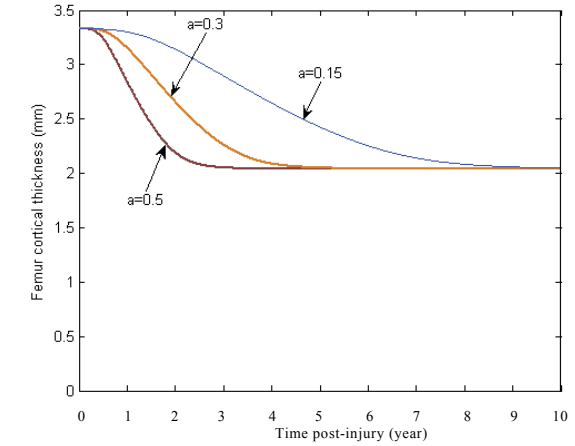

(a)

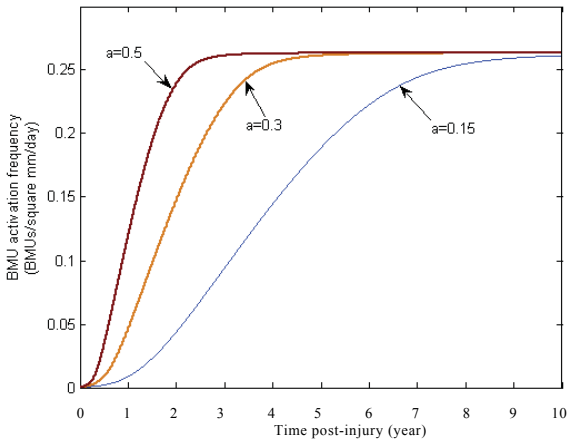

(b)

Figure 6: Effects of varying the decreasing coefficient a of mechanical load [equation (7)] on cortical thickness and BMU activation frequency for femur model. (a) Cortical thickness; (b) BMU activation frequency.

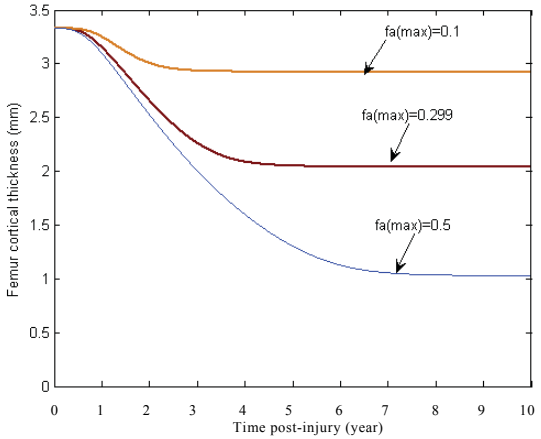

(a)

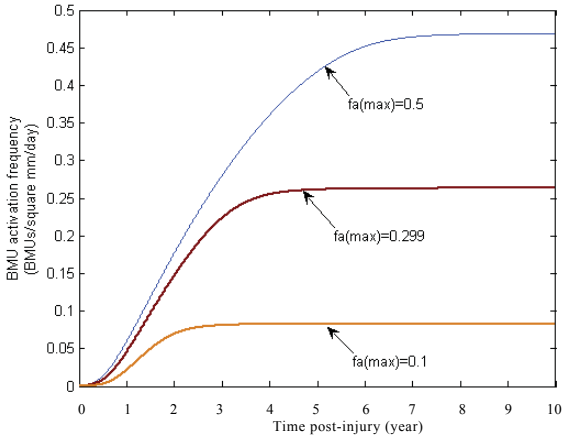

(b)

Figure 7: Effects of the maximum BMU activation frequency on cortical thickness and BMU activation frequency for femur model. (a) Cortical thickness; (b) BMU activation frequency.

Acknowledgement: This work is supported by The Hong Kong Polytechnic University Central Research Grant A/C No. G-U273 and National Natural Science Foundation of China under Grant No. 10502021.

References

1. Beaupré, G.S., Orr, T.E., Carter, D.R. (1990) An approach for time-dependent bone modeling and remodeling – application: a preliminary remodeling simulation. *J Orthop Res* 8, 662-670.

2. Currey, J.D. (1988) The effect of porosity and mineral content on the Young's modulus of elasticity of compact bone. *J Biomech* 21, 131-139.

3. Eser, P., Frotzler, A., Zehnder, Y., Wick, L., Knecht, H., Denoth, J., Schiessl, H. (2004) Relationship between the duration of paralysis and bone structure: a pQCT study of spinal cord injured individuals. *Bone* 34, 869-880.

4. Feik, S.A., Thomas, C.D.L., Clement, J.G. (1997) Age-related changes in cortical porosity of the midshaft of the human femur. *J Anat* 191, 407-416.

5. Forwood, M.R., Turner, C.H. (1995) Skeletal adaptations to mechanical usage: results from tibial loading studies in rats. *Bone* 17, 197s-205s.

6. Frost, H.M. (1983) A determinant of bone architecture: the minimum effective strain. *Clinical Orthopaedics Related Research* 175, 286-292.

7. Frost, H.M. (2000) Does bone design intend to minimize fatigue failure? A case for the affirmative. *J Bone Mineral Metab* 18, 278-282.

8. Ganong, W.F. (2005) In *Review of medical physiology* [electronic resource] (Lange Medical Books/McGraw-Hill. New York).

9. Gluer, C.-G., Cummings, S.R., Pressman, A., Li, J., Gluer, K., Faulkner, K.G., et al. (1994) Prediction of hip fractures from pelvic radiographs: the study of osteoporotic fractures. *J Bone Miner Res* 9, 671-677.

10. Gong, H., Zhang, M., Zhang, H., Zhu, D., Yang, L. (2006) Theoretical analysis of contributions of disuse, basic multicellular unit activation threshold, and osteoblastic formation threshold to changes in bone mineral density at menopause. *J Bone Miner Metab* 24, 386-394.

11. Gross, T.S., Rubin, C.T. (1995) Uniformity of responsive bone loss induced by disuse. *J Orthopaedic Res* 13, 708-714.

12. Hazelwood, S.J., Martin, R.B., Rashid, M.M., Rodrigo, J.J. (2001) A mechanistic model for internal bone remodeling exhibits different dynamic responses in disuse and overload. *J Biomech* 34, 299-308.

13. Hernandez, C.J., Beaupre, G.S., Marcus, R., Carter, D.R. (2001) A theoretical analysis of the contributions of remodeling space, mineralization, and bone balance to changes in bone mineral density during alendronate treatment. *Bone* 29, 511-516.

14. Hernandez, C.J., Beaupre, G.S., Carter, D.R. (2003) A theoretical analysis of the changes in basic multicellular unit activity at menopause. *Bone* 32, 357-363.

15. Jones, D.B., Nolte, H., Scholubbers, J.G., Turner, E., Veltel, D. (1991) Biochemical signal transduction of mechanical strain in osteoblast-like cells. *Biomaterials* 12, 101-104.

16. Lang, T., LeBlanc, A, Evans, H., Lu, Y., Genant, H., Yu, A. (2004) Cortical and trabecular bone mineral loss from the spine and hip in long-duration spaceflight. *J Bone Miner Res* 19, 1006-1012.

17. LeBlanc, A., Shackelford, L., Schneider, V. (1998) Future human bone research in space. *Bone* 22, 113s-116s.

18. Martin, R.B. (2000) Towards a unifying theory of bone remodeling. *Bone* 26, 1-6.

19. Mullender, M.G., Huiskes, R. (1995) A proposal for the regulatory mechanism of Wolff's law. *J Orthop Res* 13, 503-512.

20. Paga, A., Jasty, M., Bragdon, C., Ito, K., Harris, W.H. (1991) Alterations in femoral and acetabular bone strains immediately following cementless total hip arthroplasty: an in vitro canine study. *J Orthop Res* 9, 738-748.

21. Parfitt, A.M. (1983) The physiologic and clinical significance of bone histomorphometric data. In *Bone histomorphometry: techniques and interpretation*, ed. Recker, R.R. (CRC Press, Boca Raton, FL), pp. 143-223.

22. Prince, R.L., Price, R.I., Ho, S. (1988) Forearm bone loss in hemiplegia: a model for the study of immobilization osteoporosis. *J Bone Miner Res* 3, 305-310.

23. Ritzel, H., Amling, M., Pösl, M., Hahn, M., Delling, G. (1997) The thickness of human vertebral cortical bone and its changes in aging and osteoporosis: a histomorphometric analysis of the complete spinal column from thirty-seven autopsy specimens. *J Bone Miner Res* 12, 89-95.

24. Slade, J.M., Bickel, S., Modlesky, C.M., Majumdar, S., Dudley, G.A. (2005) Trabecular bone is more deteriorated in spinal cord injured versus estrogen-free postmenopausal women. *Osteoporosis Int* 16, 263-272.

25. Turner, C.H., Anne, V., Pidaparti, R.M.V. (1997) A uniform strain criterion for trabecular bone adaptation: do continuum-level strain gradients drive adaptation? *J Biomech* 30, 555-563.

26. Turner, C.H., Forwood, M.R., Rho, J.Y., Yoshikawa, T. (1994) Mechanical loading thresholds for lamellar and woven bone formation. *J Bone Miner Res* 9, 87-97.